Biochemical Engineering Journal 15 (2003) 165–175

Biochemical Engineering Journal

www.elsevier.com/locate/bej

An integrated hybrid neural system for noise filtering, simulation and control of a fed-batch recombinant fermentation☆

P.R. Patnaik*

Institute of Microbial Technology, Sector 39-A, Chandigarh 160 036, India

Received 1 February 2002; received in revised form 20 November 2002; accepted 20 November 2002

Abstract

Fermentations employing genetically modified (recombinant) bacteria have complex metabolisms that are sensitive to the operating conditions. Therefore it is difficult to propose simple and accurate mathematical models suitable for industrial conditions. Under such a simulated condition, a fed-batch fermentation has been analyzed here for recombinant β-galactosidase production by *Escherichia coli* containing the plasmid pOU140. A previous study had shown that representing the bioreactor by an Elman neural network and coupling this to neural networks to filter the disturbances selectively and to control the fermentation generated more β-galactosidase than a well-mixed, noise-free fermentation. To overcome the limitations of large recurrent networks, the bioreactor has now been represented by a hybrid model which combines a partial mathematical model with two small Elman neural networks for the intra-cellular variables, an autoassociative network to filter the noise and a feedforward network as the controller. This integrated system permits more robust operation in the presence of disturbances and produces smoother profiles of the concentrations, improved gene expression and more β-galactosidase than previously achieved with an Elman network alone.

Keywords: Recombinant fermentation; Fed-batch; Nonideal condition; Hybrid neural network

1. Introduction

Measurements, modeling and control of industrial scale microbial fermentations are difficult and expensive, largely due to the difficulties is the loss of some of the ideal features associated with small laboratory-scale reactors. These include the influx of external disturbances, particularly those carried by the feed streams, significant spatial gradients in large vessels, and transport limitations [1]. Transport resistances may be overcome in small reactors but in large vessels they can seriously impede the performance, especially when two or more phases are involved, as in aerated broths or those employing immobilized cells or enzymes. Spatial variations in large bioreactors require more measuring probes for comprehensive data generation, thus increasing the cost and interfering with fluid circulation [2].

Owing to their high sensitivities, fermentations employing genetically modified (recombinant) cells pose additional problems [3]. Recombinant broths contain two kinds of cells: (a) recombinant cells, which harbor plasmids introduced from another organism and (b) plasmid-free cells. Their growth rates differ and only plasmid-harboring cells have the genetic mechanism to synthesize a product of interest. Disturbances as well as heterogeneity of the broth affect the recombinant (plasmid-containing) cells and plasmid-free cells in different ways. In addition, while all the cells in a shaken flask or a small bioreactor may contain the same number of copies of the plasmid, there can be substantial variations in the copy number among the population of cells in a large bioreactor [4,5], and the particular distribution of the copy number can have a significant effect on protein synthesis [6,7].

Classical bioreactor theory teaches that it is preferable that all recombinant cells in a fermentation broth have the same number of plasmids and the broth should be perfectly isotropic. However, since neither objective can be fully realized on a practically useful scale of operation, an alternate approach is to optimize the distribution of the plasmid copy number and the degree of mixing of the broth; indeed, such optimal nonideal performance may yield more of the recombinant protein than an ideal bioreactor [6–8].

While optimal filtering of noise and control of mixing and the copy number distribution may enhance the performance, they also make it more difficult and expensive to employ

☆ IMTECH communication no. 006/2001.

* Fax: +91-172-690585/690632.
E-mail address: pratap@imtech.res.in (P.R. Patnaik).

1369-703X/02/$ – see front matter © 2002 Elsevier Science B.V. All rights reserved.
PII: S1369-703X(02)00195-X

Nomenclature

D	overall dilution rate (l/h)
D_a	axial dispersion coefficient (cm^2/h)
D_j	internal dilution rate for jth region (l/h)
k_1, k_2, k_3, k_4	reaction rate constants (l/h)
K, K_1, K_2, K_p	equilibrium constants (g/l)
L	characteristic length for bioreactor (cm)
Q	substrate feed rate (l/h)
Q_1	internal flow rate from region 1 to region 2 (l/h)
Q_2	internal flow rate from region 2 to region 1 (l/h)
r^+_{Aj}, r^-_{Aj}	rates of change of A-compartments in jth region (l/h)
r^+_{Ej}	rate of change of E-compartment in jth region (l/h)
r^+_{Gj}, r^-_{Gj}	rates of change of G-compartments in jth region (l/h)
r^+_{Pj}	rate of change of P-compartment in jth region (l/h)
s_j	S_j/S_0 (dimensionless)
S_0	initial substrate concentration in bioreactor (g/l)
S_f	substrate concentration in the feed stream (g/l)
S_j	substrate concentration in jth region (g/l)
t	time (h)
u	fluid velocity (cm/h)
v_1	V_1/V (dimensionless)
V	total volume of the broth (l)
V_j	volume of broth in jth region ()
x	X/S_0 (dimensionless)
x^+	$x^+_1 + x^+_2$ (dimensionless)
x^-	$x^-_1 + x^-_2$ (dimensionless)
x^+_{Aj}, x^-_{Aj}	concentrations of A-compartments in jth region (g/g)
x^+_{Ej}	concentration of E-compartment in jth region (g/g)
x^+_{Gj}, x^-_{Gj}	concentrations of G-compartments in jth region (g/g)
x^+_j	X^+_j/S_0 (dimensionless)
x^-_j	X^-_j/S_0 (dimensionless)
x^+_{Pj}	concentration of P-compartment in jth region (g/g)
X	overall biomass concentration in bioreactor (g/l)
X^+_j	concentration of plasmid-bearing cells in jth region (g/l)
X^-_j	concentration of plasmid-free cells in jth region (g/l)
$Y_{x/s}$	yield coefficient for biomass from substrate (g/g)

Greek symbols

γ_{11}, γ_{22}	stoichiometric coefficients for intra-cellular reactions (dimensionless)
Δ_j	Q_j/V_1 (l/h)
θ	plasmid loss probability (dimensionless)
μ	overall specific growth of biomass (l/h)
μ_j	overall specific growth rate in jth region (l/h)
μ^+_j, μ^-_j	specific growth of cells in jth region (l/h)
σ^+_j, σ^-_j	intra-cellular substrate concentration in jth region (g/l)
τ	tD (dimensionless)
φ	mass fraction of recombinant cells (dimensionless)
ω	V_2/V_1 (dimensionless)

Superscripts

+	plasmid-containing cells
−	plasmid-free cells

sensors to monitor the performance and to apply mathematical models and model-based control. Artificial neural networks (ANNs) then offer a viable alternative. Recent reviews [9,10] have shown that ANNs are superior to mathematical models and to nonparametric methods such as the extended Kalman filter, and they may be employed both to simulate a fermentation and to provide dynamically optimal filtering of the noise present in a feed stream [11].

Because ANNs function as 'black box' representations of a process, their performance depends strongly on how they are trained, the choice of data and the method of training. Just as an inadequately or improperly trained network does not learn enough about a process, excessive training makes the network learn spurious features which impair its performance [12]. The topology of an ANN also has a profound effect on its performance. Like over-learning, too many layers or too many neurons in a particular layer may undermine the efficiency of a network rather than improve it [13].

These difficulties limit the practical usefulness of ANNs for recombinant fermentations in real applications. So, by combining mathematical models of some features of a fermentation with neural networks for those features which are difficult to model, hybrid neural networks (HNNs) (Fig. 1) provide a balance between the two approaches. Fig. 1 is of course a simplified picture, and in a real application the HNN may include many models and many networks with interactions among them [14,15].

The usefulness of HNNs has been demonstrated in many laboratory scale fermentations [14,16–19]. However, these applications used simple nonoptimal configurations, which

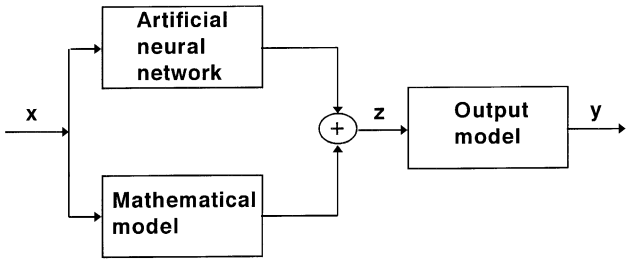

Fig. 1. Structure of a hybrid neural network: *x*—inputs; *z*—internal outputs; *y*—processed usable outputs.

may not be adequate for the nonideal features of an industrial fermentation, where the usefulness of HNNs are fully realized. In a study that forms the basis of the present work, Patnaik [20] simulated a fed-batch industrial scale fermentation for β-galactosidase from recombinant *Escherichia coli* by 'corrupting' an ideal, deterministic model with imperfect mixing and Gaussian noise in the flow rate of the substrate feed stream to a fed-batch bioreactor. It was shown that an HNN mimicked the time-domain profiles of the concentrations of recombinant cells, plasmid DNA and β-galactosidase more accurately than an ANN. The present work extends that study to a hybrid neural control system where ANNs for filtering of inflow noise, control of the bioreactor and simulation of some properties of the fermentation are combined with partial mathematical models to design an integrated HNN for simulation and control.

2. Model development and data generation

For consistency and comparison, the fermentation system was the same as that studied before [21–24]. This is the production of β-galactosidase by *E. coli* CSH50 harboring the plasmid pOU140. The expression of β-galactosidase is induced by temperature. Below a threshold temperature (37 °C), the plasmid replicates very slowly, whereas above this temperature there is a dramatic increase in the replication rate, and the plasmid copy number increases up to a 100-fold. To maintain a healthy production rate without over-burdening the cells, Betenbaugh et al. [25] and Nielsen et al. [26] proposed operating the bioreactor for short (optimal) durations alternately above and below 37 °C. Initially a sufficiently large concentration of plasmids per cell is allowed to be formed; before this concentration becomes metabolically unsupportable, the temperature is lowered below 37 °C and the fermentation continued until the copy number becomes too small, where upon the temperature is raised again.

However, this cyclic temperature operation adds to the difficulties of large bioreactors, and carries the risk of inducing runaway behavior. Extending his earlier work [20], Patnaik [27] showed that by maintaining an optimal time-dependent degree of incomplete mixing it is possible to avoid temperature cycling and sustain the fermentation productively for long durations (20–30 h) below 37 °C. This result allows two advantages. First, it removes the risks of fatal metabolic loads and runaway behavior. Secondly, it enables the normal incomplete mixing in large bioreactors to be gainfully exploited to improve productivity.

Previous studies [20,24,27] and this one utilized the kinetic models proposed earlier [25,26] for fermentation below 37 °C. The model was based on a conceptual division of an *E. coli* cell into four compartments (Fig. 2(a)). Compartment A contains mRNA, tRNA and ribosomes; presumably because of their key roles in the metabolism, the recombinant DNA and the plasmid-encoded protein (β-galactosidase) were assigned separate compartments, P and E, respectively; the rest of the cellular material, including genomic DNA, was lumped into a G-compartment. Signal flows inside a cell are indicated in the figure. Cells devoid of the plasmid do not have the P and E compartments. Nielsen et al. [26] proposed the kinetic equations given in the Appendix A for the rates of change of the compartments and the specific growth rates of both kinds of cells. The kinetic models for the cells and the reactor were decoupled by introducing an intra-cellular

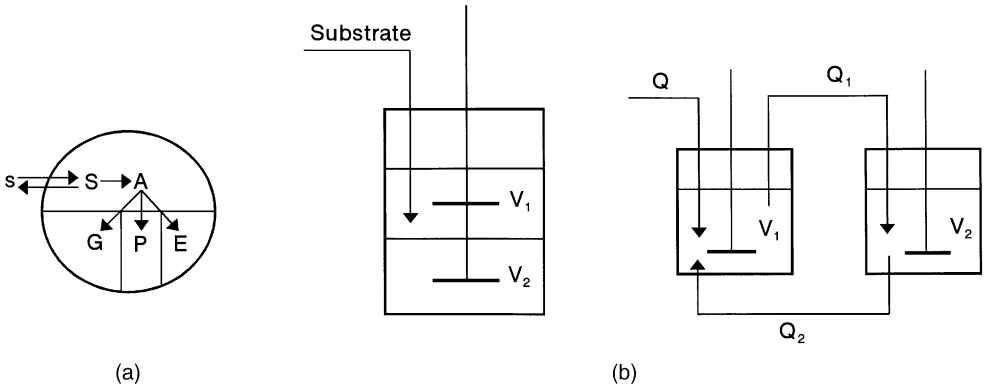

Fig. 2. Schematic diagrams for a structured cell model [26] and its application in a model for fluid mixing in a fed-batch bioreactor [27]. In (a), *s*—substrate external to the cells, *S*—substrate inside the cells, and A, G, P and E are explained in the text. Symbols in (b) are defined in the nomenclature.

substrate, S, which is in pseudo-steady state equilibrium with the extra-cellular substrate, s. The reaction $S \rightarrow$ A goes through a set of building blocks, and the conversions of A into G, P and E were considered to follow saturating kinetics.

The regulation of carbon inflow, mainly as glucose, in the substrate feed stream is a crucial aspect of the fermentation. Fermentations with *E. coli* are inhibited by acetate and the recombinant protein. Acetate formation is favored by the feeding of excessive glucose to promote high cell growth rates [28]. However, acetate itself inhibits cell growth and formation of the recombinant protein [29]. While the repression of protein formation may help bacterial growth by reducing the metabolic load [30,31], this becomes significant only if there is considerable accumulation inside the cells. Moreover, a large proliferation of cells and poor generation of the desired protein is of little use. Many studies [27,32,33] have shown that this is best achieved by fed-batch operation; so the bioreactor model shown in Fig. 2(b) is for a fed-batch process. In this model, macromixing is described by a combination of two continuous flow stirred tanks (CFSTRs), explained in an earlier work [27]. The two CFSTRs denote two regions of the broth, one enclosing the point of introduction of the inoculum and the substrate feed stream (region 1) and the other away from this (region 2). Each region is considered to function as a CFSTR, whose dilution rate D_i ($i = 1$, 2) is a measure of the degree of mixing in that region. There is also a dilution rate, D. If D_1 or D_2 is large, that region has intense mixing, while a low D_i indicates poor mixing. In the limiting cases, $\{D_1, D_2 \rightarrow \infty\}$ indicates a perfectly mixed broth, while $\{D_1, D_2 \rightarrow 0\}$ denotes completely segregated flow. In real situations D_1 and D_2 are likely to have finite non-zero values. All three dilution rates and the kinetic equations are defined in the Appendix A, where it may be seen that the intra-cellular and extra-cellular processes are linked by transport across the cell walls as described by Nielsen and Villadsen [34].

Since practical difficulties and commercial restrictions limit the scope of data that can be obtained from an industrial bioreactor, many authors [14,19,35,36] have found it useful to generate data simulating an industrial fermentation by adding noise to a deterministic model. Using this approach and observations that disturbances associated with large bioreactors may be described by a mixture of Gaussian distributions with different variances and with a time-dependent mean equal to the instantaneous value of the noise-affected variable [11,37,38], data simulating an industrial fermentation were generated by solving the equations in the Appendix A, both without and with Gaussian noise in the feed stream. For each flow rate, variances spanning 0–20% were employed [20,24]. Although a constant interval is simple to implement, it may generate too many points in regions where the variables change slowly and too few data in regions with sharp gradients. Based on previous experience [11,21], the sampling interval was varied according to the local gradient of the concentration of β-galactosidase.

3. Development of the HNN control system

Because of the critical effect of the substrate feed rate, disturbances in this flow rate have a direct impact on cell metabolism and product formation. While static filters (such as the Butterworth or the Kalman type) are commonly used to prune any inflow noise, it is difficult to program them to respond dynamically to disturbances with mixed time-dependent distributions. This can be done more readily by trained neural networks, such that the neurally filtered stream contains noise of a prescribed time-dependent mean and variance [11,22,36]. Since the input and output variables of the filter are the same, an autoassociative ANN is a suitable choice for the filtering device [9,12].

In a previous study [21] it has been shown that an Elman neural network (Fig. 3) provides a better representation of this fermentation than a feed-forward ANN with prefixed transform functions, employed by others [37,39]. The main reason for this superiority is the presence of recurrent neurons in the Elman ANN, which provide internal feedback of information accounting for hydrodynamic interactions in a nonhomogeneous broth [21,24]. While the internal feedback feature helps a recurrent ANN to portray a nonideal bioreactor, it also increases the training effort. So, a prudent approach is to combine Elman networks for some variables with mathematical models for others. When intra-cellular kinetics are known, as in the present case, the postulated rate equations may be used. Two key variables which are difficult to measure and model in large bioreactors are the rates of cell growth and the plasmid DNA content because cells dispersed in the broth differ in age, plasmid content and growth rates [4,5,30], and there are no clear transitions between the lag, exponential and stationary phases of growth. So these two concentrations are good candidates for on-line estimates by Elman neural networks. Since the specific growth rate is a function of the cell concentration, a more fundamental

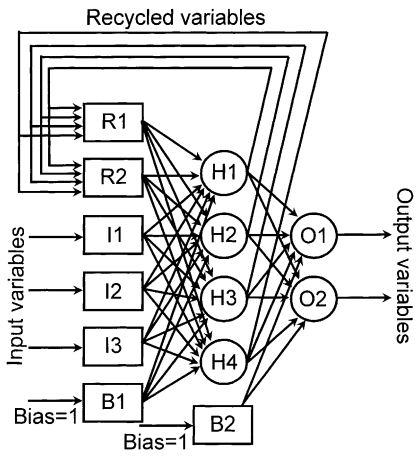

Fig. 3. Topological structure of an Elman neural network. I1, I2, I3: input neurons; H1, H2, H3, H4: hidden neurons; O1, O2: output neurons; B1, B2: bias neurons; R1, R2: recurrent neurons.

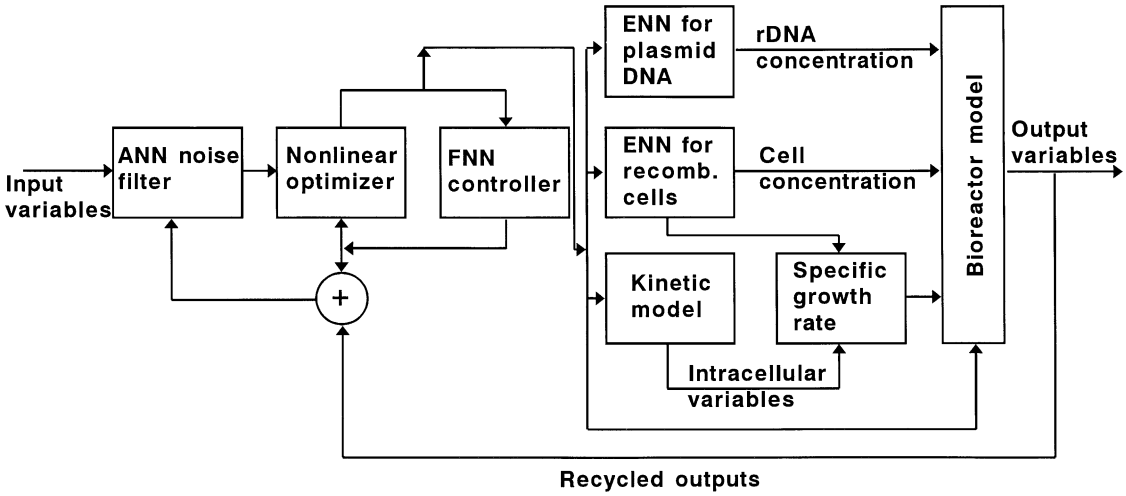

Fig. 4. Signal flow diagram for hybrid neural simulation, filtering and control of a fed-batch bioreactor. ANN: autoassociative neural network; ENN: Elman neural network; FNN: feed forward neural network.

property, the latter variable is preferred for neural representations [14,16,17].

Two recent studies of fed-batch fermentation for recombinant β-galactosidase indicate that an HNN combining two Elman neural networks with differential equations for intra-cellular kinetics and macroscopic balances for the bioreactor [20] represents simulated data of a nonideal bioreactor more closely than when an Elman network alone [21] is employed. Fig. 4 combines this HNN configuration with a feed-forward neural controller. The choice of topology for the controller is supported by this author's work [22,24] and those of others [18,19,40]. Although the full model shown in the Appendix A contains 16 dependent variables, just five constitute the minimal set to portray the dynamics [41]. These are the concentrations of recombinant cells, total biomass, substrate, plasmid DNA and the recombinant protein (β-galactosidase). So the autoassociative neural filter has these variables and the flow rate of substrate as the inputs and outputs. Since the inputs to the ENNs are the outputs of the filter, each ENN has six input neurons; while the ENN for plasmid DNA has just one output variable, that for the recombinant cells has two output neurons, one for their concentration and the other for the mass fraction. The latter two variables automatically provide the total concentration of the biomass. For each ENN, the number of recurrent neurons and hidden neurons were varied until the sum of the squares of the differences between the training data and the predicted values was minimized. This method resulted in a 8(2)-4-1 configuration for the plasmid DNA network and 8(2)-6-2 for the ENN of the recombinant cells [20]; the numbers in each set refer to the input (recurrent), hidden and output neurons. A 5-7-3 topology was determined to be the best for the neural controller. Unlike the ENNs, a feed-forward ANN has no recurrent neuron. Note also that the number of neurons in the input layer is 5 and not 6 because the feed rate (expressed as the dilution rate, D) is an output variable here, the other two outputs being D_1 and D_2.

The controller straddles two closed loops, one containing the neural filter and the other the nonlinear optimizer; this arrangement is modified from that used by Baughman and Liu [42] to include the effect of any recycled outputs. Studies with different strains of recombinant *E. coli* [23,33,39] have shown that maximizing the productivity piecewise during successive intervals of time generates a better performance than maximizing the end-point concentration. Thus, the optimization box utilizes the data during each sampling interval to determine the values of the weights of the neural controller that will maximize β-galactosidase concentration during the next interval. The controller translates the updated weights into manipulation of the three dilution rates, D, D_1 and D_2, thus regulating the feed rate and the mixing condition in the broth. Manipulation of the dilution rates also provides a better performance in terms of stability [43] and sensitivity [44] than is possible by manipulation of the feed concentration.

4. Results and discussion

In fermentations with recombinant microorganisms, four main variables are of interest. One is the cloned-gene product itself: β-galactosidase in the present case. As explained earlier, its rate of formation depends on the concentrations of the substrate, recombinant cells and plasmid DNA. These four variables therefore characterize the performance of a fermentation, and their time-domain profiles have been plotted in Figs. 5–8.

Each figure has the concentration profiles for (1) a fermentation without control and filtering of noise, (2) with neural filtering and control applied to a bioreactor represented purely by an Elman ANN and (3) with neural filtering

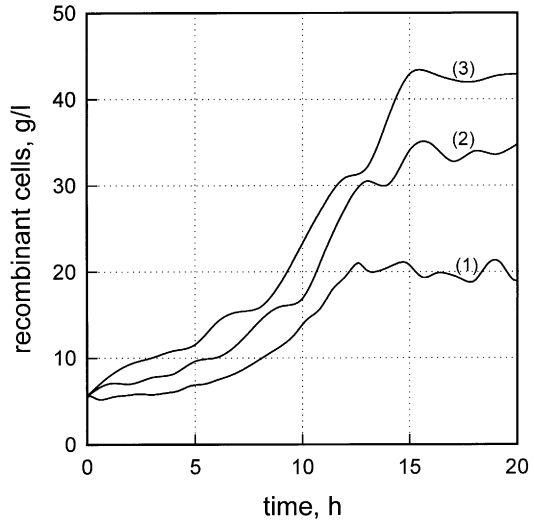

Fig. 5. Evolution of the concentration of recombinant cells with time: (1) no filtering or control, (2) neural filtering and control with an Elman neural network for the bioreactor, and (3) neural filtering and control with a hybrid neural representation of the bioreactor.

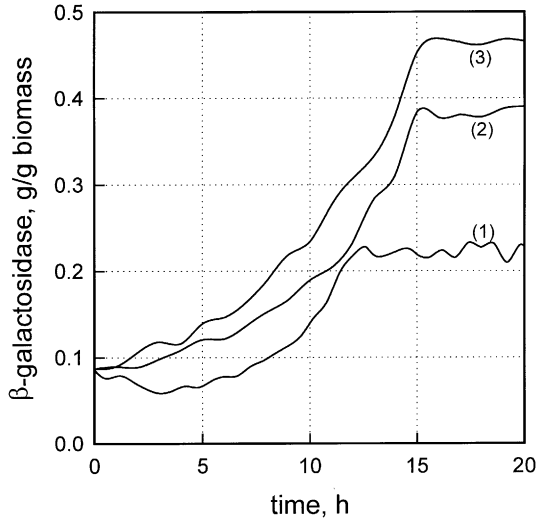

Fig. 7. Time-domain profiles of recombinant β-galactosidase concentration for each of the cases explained in Fig. 5.

and control but with the bioreactor represented by a HNN. There are other possibilities such as (a) only neural filtering or neural control and (b) conventional (PID) control with or without filtering of noise, but an earlier study [24] has shown that these combinations are inferior to a three-ANN system (case (2) mentioned above).

In the absence of filtering of noise and control of the bioreactor, the concentrations of recombinant *E. coli*, recombinant DNA and β-galactosidase decrease until about 5 h, then begin to rise and finally stabilize after 12 h. The decreases and consequent minima are clearly evident for rDNA and β-galactosidase but less so for the cells. Previous studies [29,30,32] have linked cell growth rates to expression of the cloned-gene protein. While this is true, the present results imply that sometimes the connection may not be manifested sufficiently strongly to rely on variations in the cell growth rate (which are easier to measure) as indicators of variations in protein formation. The relationship between the two is neither unique nor simple. While a large number of copies of a plasmid per cell enhances the rate of formation of the plasmid-encoded protein and inhibits the cell growth rate, some plasmids (for example, pBR322 in *E. coli* RL331T [45]) have the opposite effect. The effect also seems to depend on the cultivation conditions [46] and, for a given plasmid, it may differ from one strain of *E. coli* to another [31].

The addition of neural filtering and neural control improves the fermentation significantly and in more than one

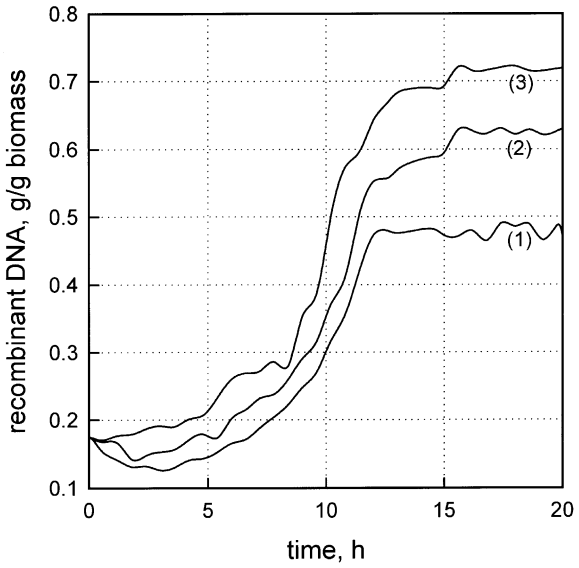

Fig. 6. Evolution of plasmid DNA concentration with time. Plots (1), (2) and (3) have the same connotations as in Fig. 5.

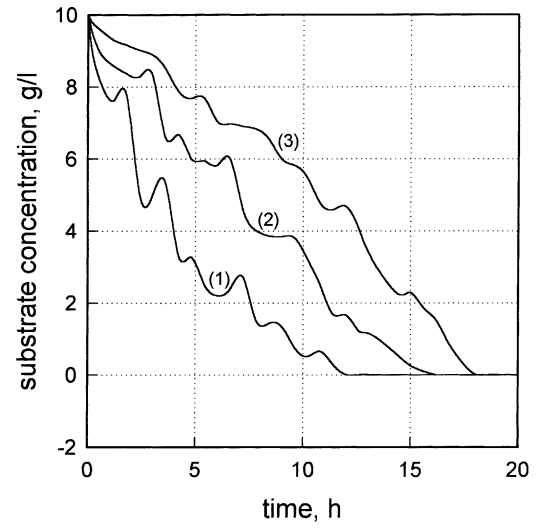

Fig. 8. Time-domain profiles of substrate (glucose) concentration for each of the cases explained in Fig. 5.

way. As expected, a hybrid model for the fermentation elicits a better performance than an Elman neural network even though both are connected (Fig. 4) to the same kinds of neural networks for noise filtering and reactor control. This improvement broadly increases with time, as evident from the observation that the ordinal distances between adjacent plots increase with time, and it is reflected in the profiles of substrate (glucose) concentration versus time. These plots (Fig. 8) offer useful insight into physiological control of the fermentation because glucose is a critical driving force, with neither insufficient nor excessive glucose being desirable [28]. Without filtering of noise and adjustment of the feed rate in response to disturbances, the optimal deterministic inflow rate [23,27] results in early depletion (within 12 h) of substrate in the bioreactor, after which further growth and β-galactosidase synthesis are derived largely from the substrate that has been assimilated by the cells. Therefore, cell growth and product formation increase only nominally when the supply of glucose can no longer match its consumption. Neural filtering and neural control of the substrate feed rate prolong the availability of the substrate, while still preventing inhibitive accumulation (and the Crabtree effect), and this is improved further by hybrid control.

An HNN representation for the fermentation also generates a less fluctuating performance. Herein we may appreciate the significance of providing feed-back between the filter, the controller and the bioreactor as shown in Fig. 4. Even though the neural topologies of the filter and the controller do not change, their performance is linked to that of the bioreactor model. Since a HNN is a more faithful depiction of the simulated bioreactor than is an Elman network alone, this has a synergestic effect on the adaptation and response of the other two neural nets. This type of cooperative performance is particularly important for unsteady state processes, implying that it is more critical for batch and fed-batch fermentations than for a continuous fermentation. In addition to generating more β-galactosidase, the incorporation of filtering and control also eliminate the initial decreases seen in the concentrations in an uncontrolled process. This effect and the subsequent rise and plateauing of all three concentrations have a mechanistic connection with fluid circulation in an imperfectly mixed broth and its role vis-a-vis the movements of plasmid-bearing and plasmid-free cells [23,24].

Although it has been stated above that the concentration-time plots eventually stabilize and reach plateaus, these are not strictly constant values because of variations in the mixing intensity in the broth (as regulated by D_1 and D_2) and in the incoming noise. However, the "steady state" fluctuations reduce upon moving from (a) the absence of control and filtering to (b) controlled fermentation with an Elman ANN for the bioreactor to (c) fermentation as in (b) but with a HNN for the bioreactor. These comparisons are quantified in Table 1. The mean values and standard deviations were calculated for the concentrations between 15 and 20 h into the fermentation, when reasonably steady fluctuations are seen (Figs. 5–8). Considering standard deviations (S.D.) as measures of dispersion of the data, it is seen that the absolute values of S.D. increase marginally from the left to the right of the table for the intra-cellular variables (rDNA and β-galactosidase) but decrease for the recombinant cell mass concentration. Nevertheless, the S.D. as a percentage of the corresponding mean value decreases upon adding a filter and a controller with, first, an Elman ANN, and further with a HNN. However, these percentages are much larger (5–10 times) than those for the recombinant cell concentration. Both differences underline the limitations of deriving quantitative conclusions about intra-cellular processes from extra-cellular measurements, even though they may be physiologically linked [29–32].

That the incorporation of a neural filter and a neural controller improve the fermentation significantly is evident from the mean "steady state" data in Table 1. With an Elman neural network, the recombinant cell concentration and that of β-galactosidase increase by more 70%, while a hybrid network achieves more than 100% enhancement in the final β-galactosidase concentration. It is notable that plasmid DNA concentration increases by one-fourth to one-half of these percentages. This implies that even though a combination of neural networks generates a modest increase in the recombinant DNA content of *E. coli* cells, it facilitates expression of the cloned-gene protein much more.

It has been suggested [11,22] that controlled filtering of inflow noise improves bioreactor performance because of resonance between the imposed frequency and the natural frequency of the system. In a fed-batch operation, the natural frequency may change with time because of changes in

Table 1
Comparison of the performances of the bioreactor with (1) no filtering or control, (2) neural filtering and control utilizing an Elman neural network and (3) neural filtering and control coupled to a hybrid model

Performance indicator	Unfiltered and uncontrolled		Filtered and controlled			
	Mean value	Standard deviation	Elman neural network		Hybrid neural model	
			Mean value	Standard deviation	Mean value	Standard deviation
Recombinant cells (g/l)	19.81	0.792 (4.0%)	33.98 [71.5%]	0.777 (2.3%)	42.63 [115.2%]	0.616 (1.4%)
Recombinant DNA (g/g biomass)	0.306	0.0736 (24.0%)	0.359 [17.3%]	0.0763 (21.2%)	0.448 [46.4%]	0.0874 (19.5%)
β-Galactosidase (g/g biomass)	0.222	0.0517 (23.3%)	0.383 [72.5%]	0.0802 (20.9%)	0.464 [109.0%]	0.0872 (18.8%)

Note: The figures in parentheses are the standard deviations as percentages of the mean values; those in square brackets are the percentage increases over the corresponding values for an uncontrolled fermentation (column 2).

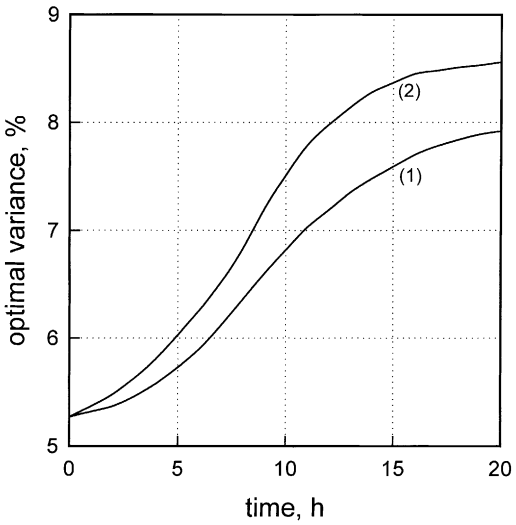

Fig. 9. Comparison of the profiles of optimal variances of the filtered noise for (1) an Elman neural network and (2) a hybrid neural model for the bioreactor.

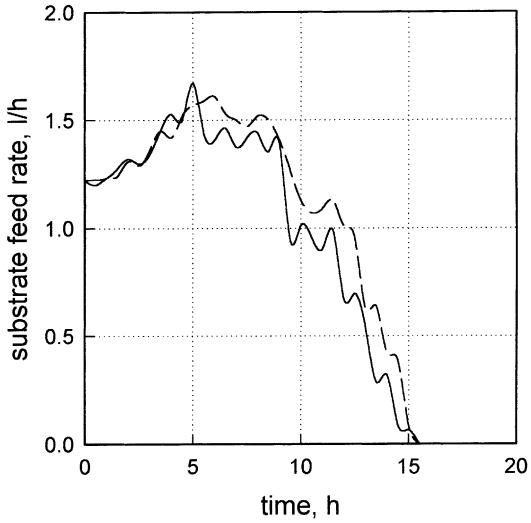

Fig. 10. Comparison of the substrate feed rates after neural filtering for the bioreactor represented by an Elman neural network (broken line) and a hybrid neural model (continuous line).

the volume of the broth, its rheological properties, cell concentrations and, in large vessels, the mixing pattern. Therefore the frequency (reflected in terms of the variance of the filtered noise) in the filtered feed stream should also vary with time. The nonlinear optimizer (Fig. 4) determines for each inter-sample interval the variance that will maximize β-galactosidase concentration during that interval. The parameters of the neural filter are then adjusted accordingly.

Fig. 9 compares the time-dependent variation of the optimal variances for Elman and hybrid representations of the bioreactor. While the Elman configuration requires the optimal variance to increase from 5.3 to 7.9% over the 20-h fermentation period, a hybrid configuration allows a wider variation (5.3 to 8.6%). This may be interpreted to mean that a HNN permits more robust operation because less stringent filtering of inflow disturbances is required. Increases in the variance by 50 and 62%, respectively, in these cases suggest that previous designs [11,22] of neural filters for constant throughput variances were unreasonably approximate.

These differences are also reflected in the optimal feed rates of substrate determined for an Elman representation and a hybrid representation (Fig. 10). In conformity with the larger allowable variances in the inflow noise, a neural control system based on an HNN permits a more fluctuating flow rate whereas an Elman model requires more stringent filtering and control for a smoother profile. However, the wider fluctuations with an HNN-based filter do not impair the intra-cellular concentration profiles of rDNA and β-galactosidase (Figs. 6 and 7). This feature may be understood with reference to the cell model in Fig. 2(a). The externally supplied substrate first equilibrates with the intra-cellular substrate and is then converted to the components of compartment A. The equilibrium and the dominant size of A, which comprises about 60% of the cell mass [26], provide a buffer that absorbs much of the noise before the reactions proceed further to the G, P and E compartments. Since both flow profiles begin and end at the same instants of time and the Elman profile is consistently above that for an HNN, the cumulative inflow of substrate is more in the former case. This surplus substrate dilutes the broth and may inhibit the fermentation because of acetate formation and the Crabtree effect [28,29].

5. Conclusions

Recombinant fermentations under production conditions are susceptible to imperfect mixing of the broth and noise present in the substrate feed stream. Under such conditions it is difficult to propose mathematical models that express the variations in the concentrations in a simple and accurate manner. This problem is especially severe for intra-cellular variables in time-dependent fermentations. Fed-batch operation, which is employed for many recombinant fermentations, is inherently time-dependent. In addition, the recombinant product (β-galactosidase) in the example considered here is released inside the cells.

For this fermentation system, recent work [20] has demonstrated that a hybrid neural network (HNN) provides a more faithful representation of the simulated performance in fed-batch operation than an Elman network does under conditions of imperfect mixing and Gaussian noise in the feed stream. Earlier studies [22,24] had shown that an Elman ANN in conjunction with a neural filter and a neural controller provided superior performance than even a noise-free fermentation.

Based on these studies, the present work has combined a HNN with neural networks for filtering of noise and control of the bioreactor. Results show that even though the same neural network topologies are used with an Elman ANN

and a HNN, and the neural filter coupled to a HNN results in a more fluctuating feed rate than for an Elman ANN, the HNN produces smoother profiles of both intra-cellular and extra-cellular concentrations. This difference alludes to a buffering effect inside the cells and to the significance of feedback between the bioreactor, the controller and the noise filter (Fig. 4). When the concentrations stabilize after about 15 h, a bioreactor represented by an Elman ANN produces about 70% more β-galactosidase (g/g biomass) and recombinant cells (g/l) than an unfiltered and uncontrolled fermentation, whereas a hybrid model results increases of 110–115%. The increases in plasmid DNA concentration are however between one-fourth and one-half of these values.

These differences and differences in the transient profiles suggest that, even though cell growth, plasmid content and protein synthesis are interconnected [29–32], it may be misleading to draw quantitative inferences about intra-cellular variables from extra-cellular measurements in nonideal operations. Since instrumental methods are of limited use for rapid and continual monitoring of intra-cellular variables, neural networks offer a viable alternative in industrial conditions. Their practical utility is improved when they are combined with simple and verifiable mathematical models.

Acknowledgements

This work was supported by grant number BT/PR1557/PID/25/64/99 from the Department of Biotechnology of the Government of India.

Appendix A

Patnaik [27] modified the equations proposed by Nielsen et al. [26] to make them applicable for fed-batch operation with plasmid-bearing cells present in the starting culture and segregational instability. The broth is visualized to consist of two regions, each functioning as a separate bioreactor (Fig. 1). Internal recycle streams connect the reactors to represent fluid circulation. Mixing is characterized by three dilution rates, defined below.

$$D_1 = \frac{Q + Q_2 - Q_1}{V_1}$$

$$D_2 = \frac{Q_1 - Q_2}{V_2} \tag{A.1}$$

The Q's denote flow rates and V_1, V_2 are the volumes of broth in the two conceptual reactors. Metabolic reactions take place inside the recombinant cells, there is partial reversion of plasmid-bearing cells to plasmid-free cells, and transport processes link the intra-cellular reactions to the extra-cellular broth.

A.1. Kinetic equations inside the cells

(a) Plasmid-bearing cells

$$\begin{bmatrix} \frac{dx^+_{Aj}}{dt} \\ \frac{dx^+_{Gj}}{dt} \\ \frac{dx^+_{Pj}}{dt} \\ \frac{dx^+_{Ej}}{dt} \end{bmatrix} = \frac{1}{D} \begin{bmatrix} \gamma_{11} & -1 & -1 & -1 \\ 0 & \gamma_{22} & 0 & 0 \\ 0 & 0 & \gamma_{22} & \gamma_{22} \\ 0 & 0 & 0 & \gamma_{22} \end{bmatrix} \begin{bmatrix} r^+_{Aj} \\ r^+_{Gj} \\ r^+_{Pj} \\ r^+_{Ej} \end{bmatrix} - \frac{\mu^+_j}{D} \begin{bmatrix} x^+_{Aj} \\ x^+_{Gj} \\ x^+_{Pj} \\ x^+_{Ej} \end{bmatrix} \tag{A.2}$$

where

$$\begin{bmatrix} r^+_{Aj} \\ r^+_{Gj} \\ r^+_{Pj} \\ r^+_{Ej} \end{bmatrix} = \begin{bmatrix} \frac{k_1\sigma^+_j x^+_{Aj}}{\sigma^+_j + K_1} \\ \frac{k_2\sigma^+_j x^+_{Aj}}{\sigma^+_j + K_2} \\ \frac{k_3\sigma^+_j x^+_{Aj} x_n}{\sigma^+_j + K_2} \\ \frac{k_4\sigma^+_j x^+_{Aj} x^+_{Pj}}{(\sigma^+_j + K_2)(x^+_{Pj} + K_P)} \end{bmatrix} \tag{A.3}$$

The specific growth rate is:

$$\mu^+_j = \gamma_{11} r^+_{Aj} - (1 - \gamma_{22})(r^+_{Gj} + r^+_{Pj} + r^+_{Ej}) \tag{A.4}$$

(b) Plasmid-free cells

$$\begin{bmatrix} \frac{dx^-_{Aj}}{dt} \\ \frac{dx^-_{Gj}}{dt} \end{bmatrix} = \begin{bmatrix} \gamma_{11} & -1 \\ 0 & \gamma_{22} \end{bmatrix} \begin{bmatrix} r^-_{Aj} \\ r^-_{Gj} \end{bmatrix} - \frac{\mu^-_j}{D} \begin{bmatrix} x^-_{Aj} \\ x^-_{Gj} \end{bmatrix} \tag{A.5}$$

Similar to Eqs. (A.3) and (A.4), we may write:

$$\begin{bmatrix} r^-_{Aj} \\ r^-_{Gj} \end{bmatrix} = \begin{bmatrix} \frac{k_1\sigma^-_j x^-_{Aj}}{\sigma^-_j + K_1} \\ \frac{k_2\sigma^-_j x^-_{Aj}}{\sigma^-_j + K_2} \end{bmatrix} \tag{A.6}$$

and

$$\mu^-_j = \gamma_{11} r^-_{Aj} - (1 - \gamma_{22}) r^-_{Gj} \tag{A.7}$$

In these equations, the subscript + denotes cells containing the plasmid, − denotes cells without the plasmid, and the

subscript j equals 1 or 2, depending on which mixing region is being analyzed. Eqs. (A.5) and (A.6) do not contain concentrations and rates for the P and E compartments because they are not present in nonrecombinant (plasmid-free) cells.

The overall specific growth rate of biomass in each region is the weighted sum of the growth rates for the two kinds of cells:

$$\mu_j = \left(\frac{x_j^+}{x_j^+ + x_j^-}\right)\mu_j^+ + \left(\frac{x_j^-}{x_j^+ + x_j^-}\right)\mu_j^- \tag{A.8}$$

Conservation equations relate the intra-cellular components to the overall concentrations of plasmid-free and plasmid-bearing cells.

$$x_{\mathrm{A}j}^+ + x_{\mathrm{P}j}^+ + x_{\mathrm{G}j}^+ + x_{\mathrm{E}j}^+ = x_j^+; \quad j = 1 \text{ or } 2 \tag{A.9}$$

$$x_{\mathrm{A}j}^- + x_{\mathrm{G}j}^- = x_j^-; \quad j = 1 \text{ or } 2 \tag{A.10}$$

The intra-cellular substrate concentrations, σ_j^+ and σ_j^- may also be related to the concentrations, S_j, in the medium. This, however, is not straightforward like Eqs. (A.9) and (A.10). The method has been described by Nielsen and Villadsen [34], and it leads to:

$$\sigma_j^+ = \sigma_j^- = \frac{kK_1S_j}{k_1(S_j + K)}; \quad j = 1 \text{ or } 2 \tag{A.11}$$

A.2. Bioreactor model

$$\frac{\mathrm{d}v_1}{\mathrm{d}\tau} = v_1 \tag{A.12}$$

$$\frac{\mathrm{d}x_1^+}{\mathrm{d}\tau} = \frac{Y_{x/s}}{\mu x}[\mu_1^+ x_1^+(1-\theta) + \Delta_2 x_2^+ - \Delta_1 x_1^+] - x_1^+ \tag{A.13}$$

$$\frac{\mathrm{d}x_1^-}{\mathrm{d}\tau} = \frac{Y_{x/s}}{\mu x}[\mu_1^+ x_1^+\theta + \mu_1^- x_1^- + \Delta_2 x_2^- - \Delta_1 x_1^-] - x_1^- \tag{A.14}$$

$$\frac{\mathrm{d}x_2^+}{\mathrm{d}\tau} = \frac{Y_{x/s}}{\mu x}\left[\mu_2^+ x_2^+(1-\theta) + \frac{\Delta_1 x_1^+ - \Delta_2 x_2^+}{\omega}\right] - x_2^+ \tag{A.15}$$

$$\frac{\mathrm{d}x_2^-}{\mathrm{d}\tau} = \frac{Y_{x/s}}{\mu x}\left[\mu_2^+ x_2^+\theta + \mu_2^- x_2^- + \frac{\Delta_1 x_1^- - \Delta_2 x_2^-}{\omega}\right] - x_2^- \tag{A.16}$$

$$\frac{\mathrm{d}s_1}{\mathrm{d}\tau} = (1+\omega)s_\mathrm{f} + \frac{Y_{x/s}}{\mu x}(\Delta_2 s_2 - \Delta_1 s_1) - s_1 \tag{A.17}$$

$$\frac{\mathrm{d}s_2}{\mathrm{d}\tau} = \frac{Y_{x/s}}{\omega\mu x}(\Delta_1 s_1 - \Delta_2 s_2) \tag{A.18}$$

Eqs. (A.13)–(A.18) incorporate the optimum dilution rate for fed-batch fermentations [34], $D = \mu x / Y_{x/s}$. Since x and μ, specified by Eqs. (A.20) and (A.21), vary as fermentation progresses, so does D. There is no conservation equation for β-galactosidase because it is retained inside the cells.

From a mass balance for V_2 it can be shown that:

$$\Delta_1 - \Delta_2 = \omega D \tag{A.19}$$

The total cell mass concentration, x, is calculated as:

$$x = x_1^+ + x_1^- + x_2^+ + x_2^- \tag{A.20}$$

and the overall specific growth rate is the volumetrically weighted sum of the growth rates in the two regions:

$$\mu = \frac{\mu_1 + \omega\mu_2}{1+\omega} \tag{A.21}$$

The individual specific growth rates, μ_j^+, μ_j^- and μ_j with $j = 1$ or 2, are computed according to Eqs. (A.4), (A.7) and (A.8).

References

[1] G. Larsson, M. Tornquist, E. Stahl Wernersson, C. Tragardh, H. Noorman, S.-O. Enfors, Substrate gradients in bioreactors: origin and consequences, Bioproc. Eng. 14 (1996) 281–289.

[2] B. Mayr, P. Horvat, A. Moser, Engineering approach to mixing quantification in bioreactors, Bioproc. Eng. 8 (1992) 137–143.

[3] P.R. Patnaik, Sensitivity of a recombinant fermentation with run-away plasmids: a structured analysis of the effect of dilution rate, Chem. Eng. Commun. 31 (1995) 125–140.

[4] W.E. Bentley, O.E. Quiroga, Investigtion of sub-population heterogeneity and plasmid stability in recombinant *Escherichia coli* via a simple segregated model, Biotechnol. Bioeng. 42 (1993) 222–234.

[5] H. Kuo, J.D. Keasling, A Monte Carlo simulation of plasmid replication during the bacterial division cycle, Biotechnol. Bioeng. 52 (1996) 633–647.

[6] P.R. Patnaik, Optimizing initial plasmid copy number distribution for improved protein activity in a recombinant fermentation, Biochem. Eng. J. 5 (2000) 101–107.

[7] P.R. Patnaik, Enhancement of protein activity in a recombinant fermentation by optimizing fluid dispersion and initial plasmid copy number distribution, Biochem. Eng. J. 9 (2001) 111–118.

[8] P.R. Patnaik, Incomplete mixing in large bioreactors—a study of its role in the fermentative production of streptokinase, Bioproc. Eng. 14 (1996) 91–96.

[9] G.A. Montague, A.J. Morris, Neural network contributions in biotechnology, Trends Biotechnol. 12 (1994) 312–324.

[10] P.R. Patnaik, Neural network applications to fermentation processes, in: G. Subramanian (Ed.), Bioseparation and Bioprocessing, Wiley-VCH, Weinheim, 1998 (Chapter 14).

[11] P.R. Patnaik, Improvement of the microbial production of streptokinase by controlled filtering of process noise, Process Biochem. 35 (1999) 309–315.

[12] T. Masters, Practical Neural Network Recipes in C++, Academic Press, San Diego, CA, 1993.

[13] Q. Zhang, J.F. Reid, J.B. Litchfield, J. Ren, S.-W. Chang, A prototype neural network supervised control system for *Bacillus thuringiensis* fermentations, Biotechnol. Bioeng. 43 (1994) 483–489.

[14] J. Schubert, R. Simutis, M. Dors, I. Havlik, A. Lubbert, Bioprocess optimization and control: application of hybrid modelling, J. Biotechnol. 35 (1994) 51–68.

[15] H.J.L. van Can, H.A.B. te Braake, C. Helliga, K.Ch.A.M. Luyben, J.J. Heijnen, An efficient model development strategy for bioprocesses based on neural networks in macroscopic balances, Biotechnol. Bioeng. 54 (1997) 549–566.

[16] D.C. Psichogios, L.H. Ungar, A hybrid neural network-first principles approach to process modeling, AIChE J. 38 (1992) 1499–1511.
[17] M.L. Thompson, M.A. Kramer, Modeling chemical processes using prior knowledge and neural networks, AIChE J. 40 (1994) 1328–1340.
[18] I. Dumitrache, M. Caramihai, Optimal fed-batch bioprocess control via intelligent system based on hybrid techniques, Control Eng. Appl. Inform. 3 (2001) 5–14.
[19] Y. Tian, J. Zhang, A.J. Morris, Optimal control of a fed-batch bioreactor based upon an augmented recurrent neural network model, Neurocomputing 48 (2002) 919–936.
[20] P.R. Patnaik, Hybrid neural simulation of a fed-batch bioreactor for a non-ideal recombinant fermentation, Bioproc. Biosyst. Eng. 24 (2000) 151–161.
[21] P.R. Patnaik, A recurrent neural network for a fed-batch fermentation with recombinant *Escherichia coli* subject to inflow disturbances, Process Biochem. 32 (1997) 399–400.
[22] P.R. Patnaik, Coupling of a neural filter and a neural controller for improvement of fermentation performance, Biotechnol. Techn. 13 (1999) 735–738.
[23] P.R. Patnaik, Neural control of an imperfectly mixed fed-batch bioreactor for recombinant β-galactosidase, Biochem. Eng. J. 3 (1999) 113–120.
[24] P.R. Patnaik, A simulation study of dynamic neural filtering and control of a fed-batch bioreactor under nonideal conditions, Chem. Eng. J. 84 (2001) 533–541.
[25] M.J. Betenbaugh, V.M. di Pasquantio, P. Dhurjati, Improvement of product yields by temperature-shifting of *Escherichia coli* cultures containing plasmid pOU140, Biotechnol. Bioeng. 29 (1987) 513–519.
[26] J. Nielsen, A.G. Pedersen, K. Strudsholm, J. Villadsen, Modelling fermentations with recombinant microorganisms: formulation of a structured model, Biotechnol. Bioeng. 37 (1991) 802–808.
[27] P.R. Patnaik, Dispersion-induced behavior in sub-critical opertion of a recombinant fed-batch fermentation with runaway plasmids, Bioproc. Eng. 18 (1998) 219–226.
[28] G.W. Luli, W.R. Strohl, Comparison of growth, acetate production, and acetate inhibition of *Escherichia coli* strains in batch and fed-batch fermentations, Appl. Environ. Microbiol. 56 (1990) 1004–1011.
[29] B.R. Glick, Metabolic load and heterologous gene expression, Biotechnol. Adv. 13 (1995) 247–261.
[30] W.E. Bentley, N. Mirjalili, D.C. Anderson, R.H. Davis, D.S. Kompala, Plasmid encoded protein. The principal factor in the 'metabolic burden' associated with recombinant bacteria, Biotechnol. Bioeng. 35 (1990) 668–681.
[31] J.C. Diaz Ricci, M.E. Hernandez, Plasmid effects on *Escherichia coli* metabolism, Crit. Revs. Biotechnol. 20 (2000) 79–108.
[32] W. Johnston, R. Cord-Ruwisch, M.J. Cooney, Industrial control of recombinant *E. coli* fed-batch culture: new perspectives on traditional controlled variables, Bioproc. Biosyst. Eng. 25 (2002) 111–120.
[33] K. Ye, S. Jin, K. Shimizu, Fuzzy neural network for the control of high cell density cultivation of recombinant *Escherichia coli*, J. Ferment. Bioeng. 77 (1994) 663–673.
[34] J. Nielsen, J. Villadsen, Modelling of microbial kinetics, Chem. Eng. Sci. 47 (1992) 4225–4270.
[35] R. Simutis, A. Lubbert, Exploratory analysis of biopocesses using artificial neural network based methods, Biotechnol. Prog. 13 (1997) 479–787.
[36] J. Thibault, V. van Breusegem, A. Cheruy, On-line prediction of fermentation variables using neural networks, Biotechnol. Bioeng. 36 (1990) 1041–1048.
[37] G.A. Montague, A.J. Morris, M.T. Tham, Enhancing bioprocess operability with generic software sensors, J. Biotechnol. 25 (1992) 183–204.
[38] C. Di Massimo, P.A. Lant, A. Saunders, G.A. Montague, M.T. Tham, A.J. Morris, Bioprocess applications of model-based estimation techniques, J. Chem. Technol. Biotechnol. 53 (1992) 265–277.
[39] J. Glassey, G.A. Montague, A.C. Ward, B.V. Kara, Enhanced supervision of recombinant *E. coli* fermentations via artificial neural networks, Process Biochem. 29 (1994) 387–389.
[40] Hisbullah, M.A. Hussain, K.B. Ramachandran, Comparative evaluation of various control schemes for fed-batch fermentation, Bioproc. Biosyst. Eng. 24 (2002) 309–318.
[41] P.R. Patnaik, Principal component analysis of the effect of inflow disturbances on recombinant β-galactosidase fermentation, Hung. J. Ind. Chem. 25 (1997) 261–264.
[42] D.R. Baughman, Y.A. Liu, An expert network for predictive modeling and optimal design of extractive bioseparations in aqueous two-phase systems, Ind. Eng. Chem. Res. 33 (1994) 2668–2687.
[43] M.A. Henson, D.E. Seborg, Nonlinear control strategies for continuous fermenters, Chem. Eng. Sci. 47 (1992) 821–835.
[44] P.R. Patnaik, A sensitivity approach to manipulated variable selection for control of a continuous recombinant fermentation, Chem. Eng. Sci. 56 (2001) 3311–3314.
[45] S. Lin-Chao, H. Bremer, Effect of the bacterial growth rate on replication control of plasmid pBR322 in *E. coli*, Mol. Gen. Genet. 203 (1986) 143–149.
[46] J.I. Rhee, J.C. Ricci, J. Bode, K. Schugerl, Metabolic enhancement due to plasmid maintenance, Biotechnol. Lett. 16 (1994) 881–883.